Nonlinear Alfvén Waves Near an X-Type Null Point

Student: Alex Prokopyszyn

Supervisors: Prof Hood and Prof De Moortel

What I've been doing these past 9 months

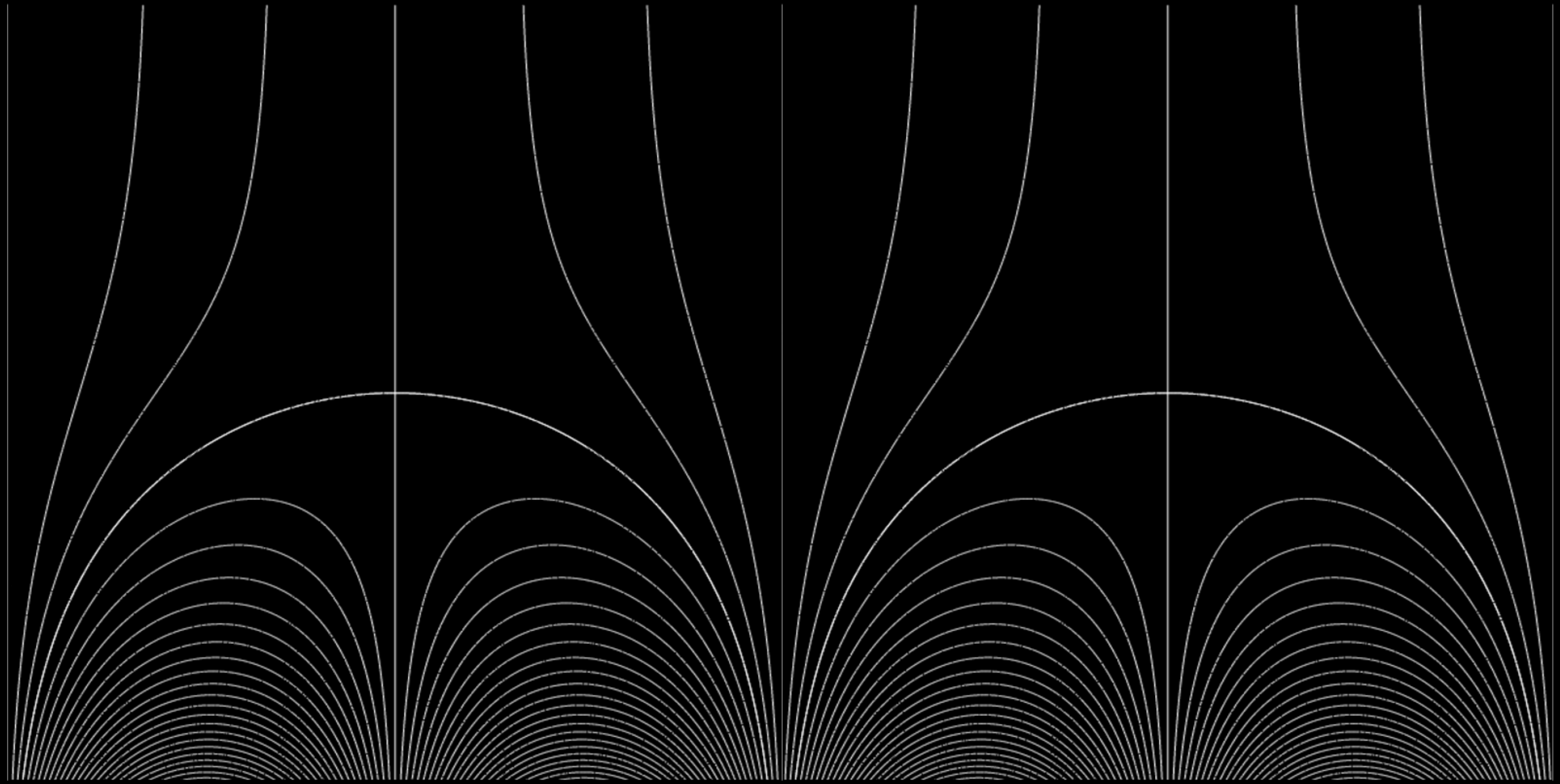

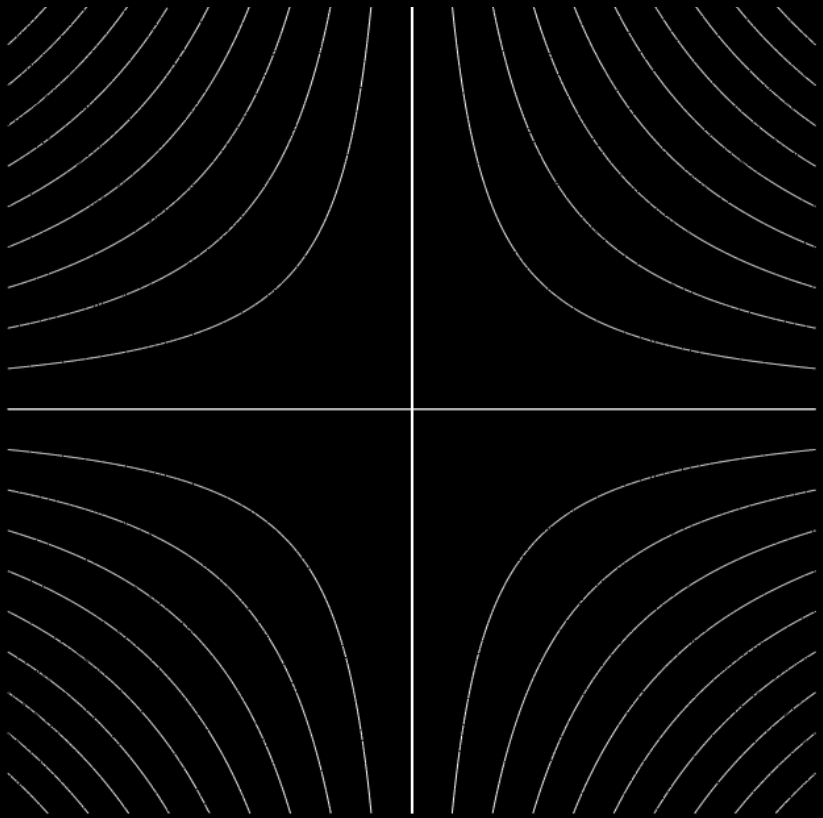

$$B_x = \sin x \; e^{-y}$$
$$B_y = 1 - \cos x \; e^{-y}$$

$$B_x = x$$
$$B_y = -y$$

Structure

- Introduction
- 1D Alfvén pulse
  - Verwichte et al. (1999)
  - Thurgood and McLaughlin (2013)
- 1D Standing Wave
  - Terradas and Ofman (2004)
- 2D X-point field
  - McLaughlin (2016)

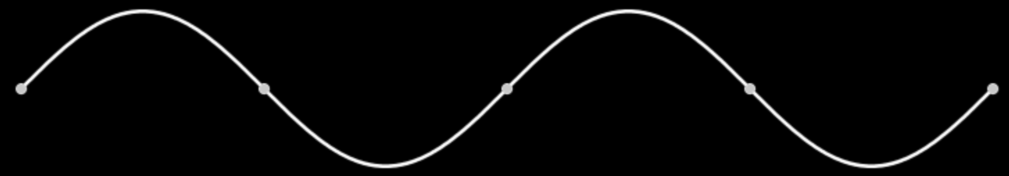

Null points

- Where $\mathbf{B} = 0$
- In 2D a separatrix is a field line which goes directly into a null point.
- Nulls are abundant in the corona

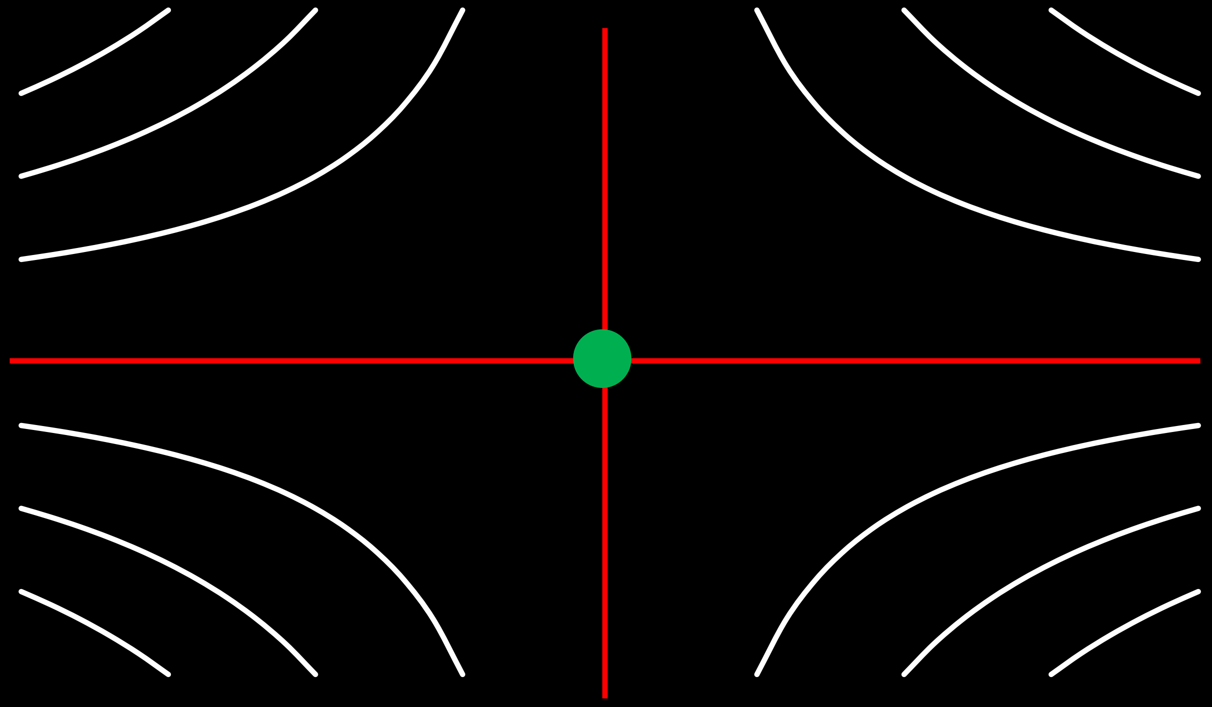

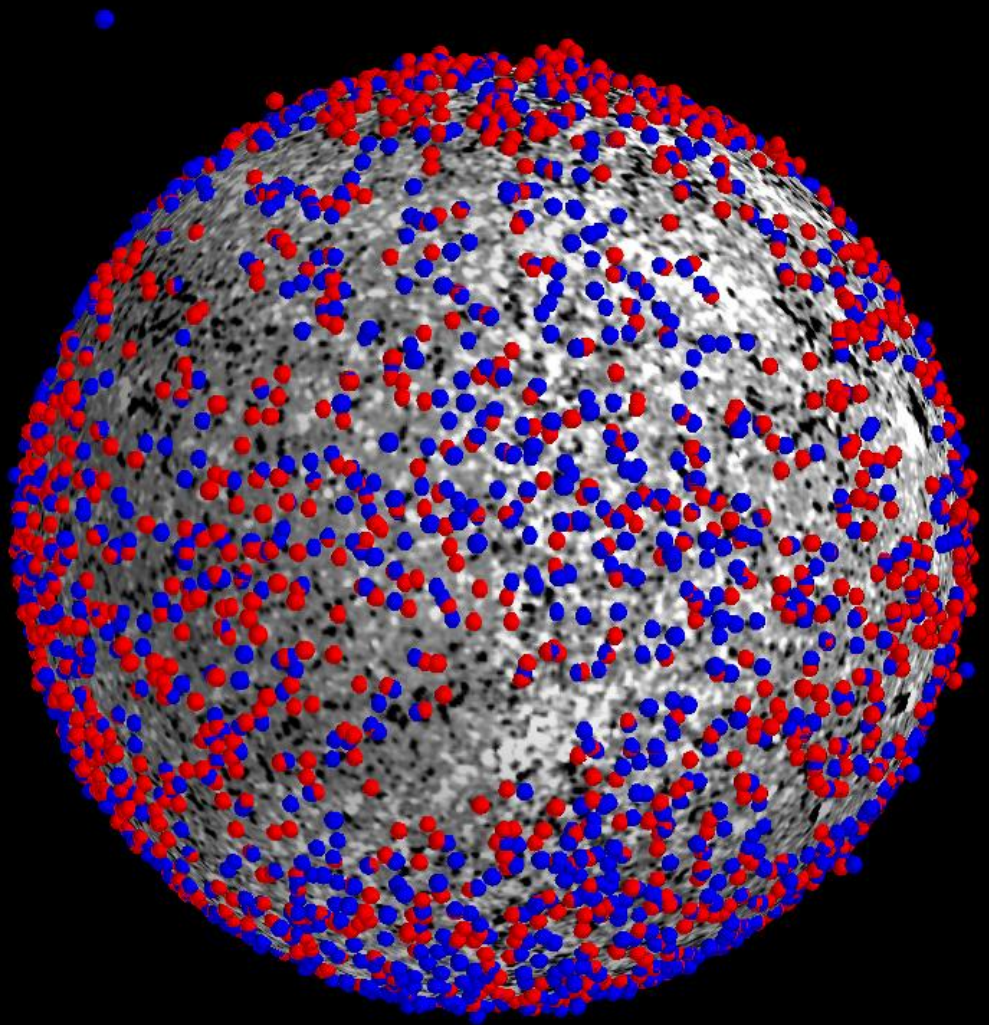

PFSS Model with $l_{max} = 641$ (Williams, 2018)

Nulls in photosphere: 693 (below 0.5Mm)
Nulls in chromosphere: 2529 (0.5Mm < R < 2Mm)
Nulls in corona: 1718 (above 2Mm)

What is a nonlinear wave?

A nonlinear wave is a wave which induces disturbances which are proportional to its amplitude squared or higher

$\underline{t = 0}$ $\underline{t > 0}$

Linear Wave:

Nonlinear Wave:

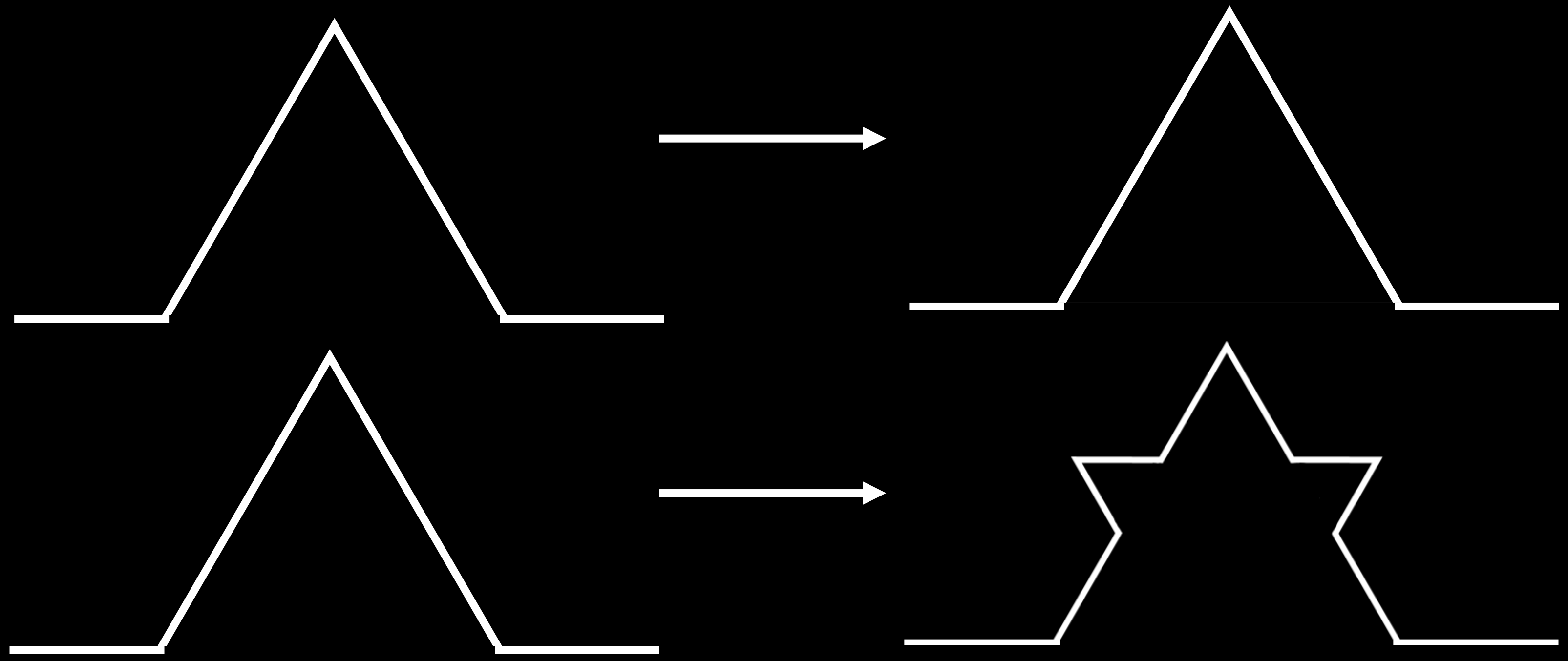

Nonlinear Wave

$\underline{t = 0}$

$$\boldsymbol{B} = \boldsymbol{B}_0 + \epsilon \boldsymbol{B}_1$$

$$\rho = \rho_0 + \epsilon \rho_1$$

$$p = p_0 + \epsilon\, p_1$$

Static Equilibrium Value

Initial Linear Wave

$\underline{t > 0}$

$$\boldsymbol{B} = \boldsymbol{B}_0 + \epsilon \boldsymbol{B}_1 + \epsilon^2 \boldsymbol{B}_2 + O(\epsilon^3)$$

$$\rho = \rho_0 + \epsilon \rho_1 + \epsilon^2 \rho_2 + O(\epsilon^3)$$

$$p = p_0 + \epsilon\, p_1 + \underbrace{\epsilon^2 p_2 + O(\epsilon^3)}_{\text{Induced Nonlinear Disturbances}}$$

Nonlinear Magnetic Pressure Force from an Alfven Wave

$\underline{t = 0}$

$$B_x = 1$$
$$B_y = 0$$
$$B_z = \epsilon e^{-x^2}$$

$$-\nabla B_z^2 = \underbrace{4\epsilon^2 x e^{-2x^2}\hat{\boldsymbol{x}}}_{\text{Nonlinear Magnetic Pressure Force}}$$

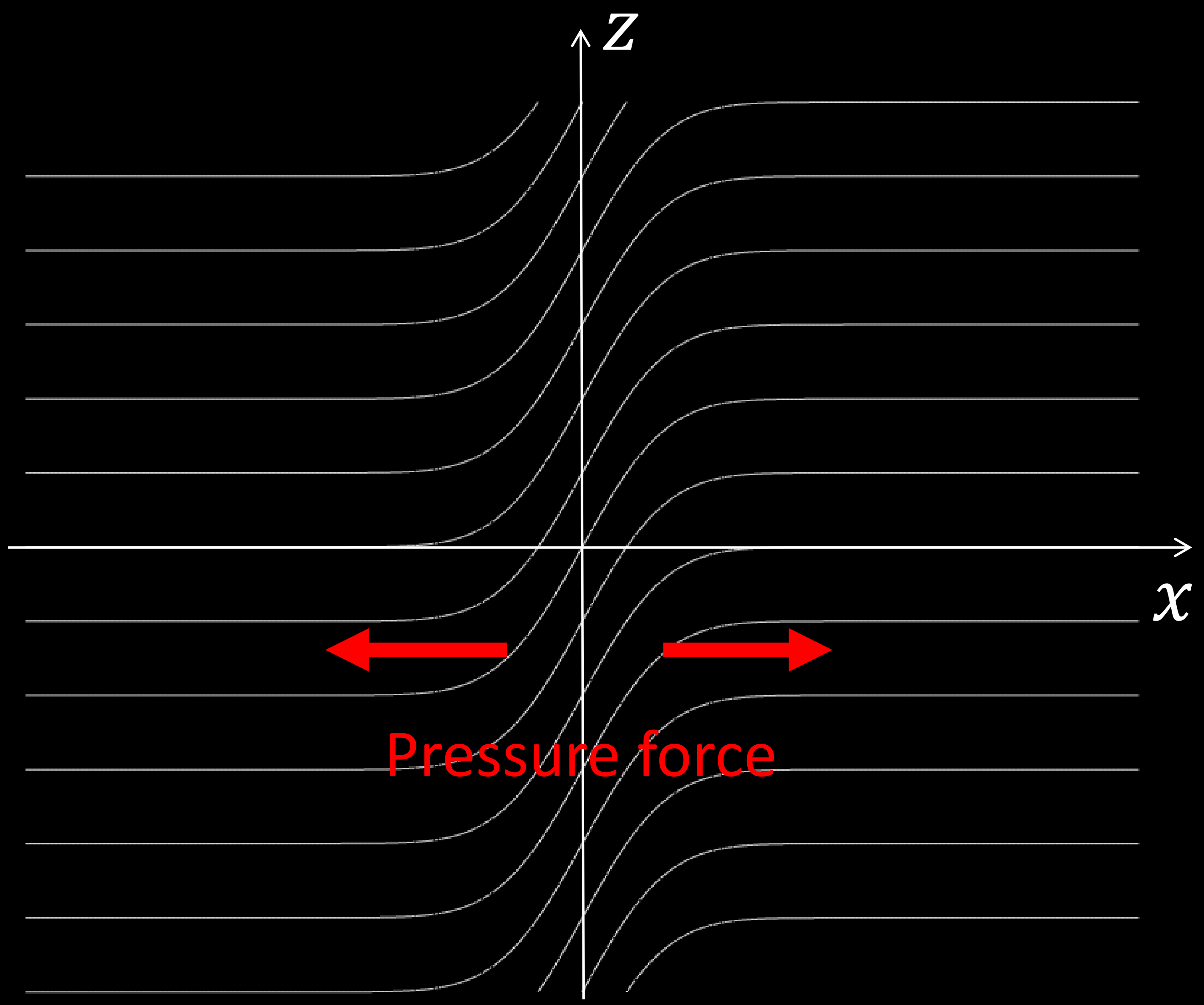

Second Order Momentum Equation for an Alfvén Wave

Conditions:

- $\beta = 0$
- $\partial/_{\partial z} = 0$
- $\nabla \times \boldsymbol{B}_0 = 0$
- $B_{z0} = 0$

Initially:

- $\boldsymbol{B}_1 = (0,0,B_{z1})$
- $\boldsymbol{v}_1 = (0,0,v_{z1})$,
- $\rho_1 = \rho_2 = \boldsymbol{B}_2 = \boldsymbol{v}_2 = 0$

$$\boldsymbol{B} = \boldsymbol{B}_0 + \epsilon \boldsymbol{B}_1 + \epsilon^2 \boldsymbol{B}_2 + O(\epsilon^3)$$
$$\rho = \rho_0 + \epsilon \rho_1 + \epsilon^2 \rho_2 + O(\epsilon^3)$$
$$\boldsymbol{v} = \epsilon \boldsymbol{v}_1 + \epsilon^2 \boldsymbol{v}_2 + O(\epsilon^3)$$

$$\boxed{\frac{\partial \boldsymbol{v}}{\partial t} = \frac{\epsilon}{\mu \rho_0} \underbrace{(\boldsymbol{B}_0 \cdot \nabla) B_{z1} \hat{z}}_{\text{Linear Tension Force}} - \epsilon^2 [\underbrace{\nabla B_{z1}^2}_{\text{Nonlinear Pressure Force}} + (\nabla \times \boldsymbol{B}_2) \times \boldsymbol{B}_0] + O(\epsilon^3)}$$

Numerical Experiment: 1D Alfvén Pulse

- Uniform $\rho_0, p_0, \boldsymbol{B}_0 = B_0\hat{\boldsymbol{x}}$
- $\boldsymbol{v}_0 = (0,0,v_{z0})$
- $\beta_0 = 0.02$
- Solid boundary conditions
- Ideal MHD

$$\frac{v_{z0}}{v_{A0}} = \begin{cases} 0.01\cos^2\dfrac{\pi x}{L_0}, & \left|\dfrac{x}{L_0}\right| \le 0.5 \\ 0, & \text{otherwise} \end{cases}$$

Numerical Experiment: 1D Alfvén Pulse

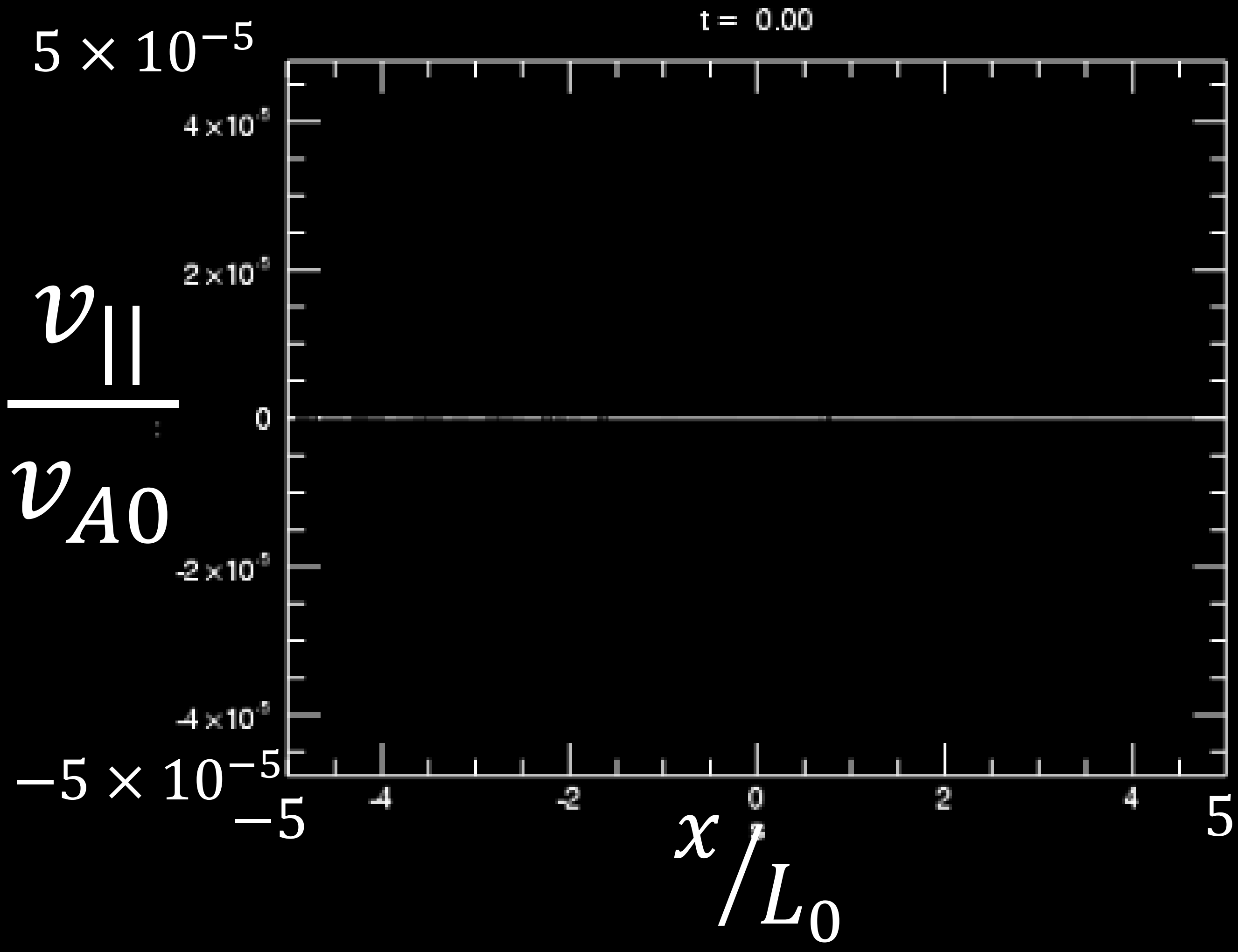

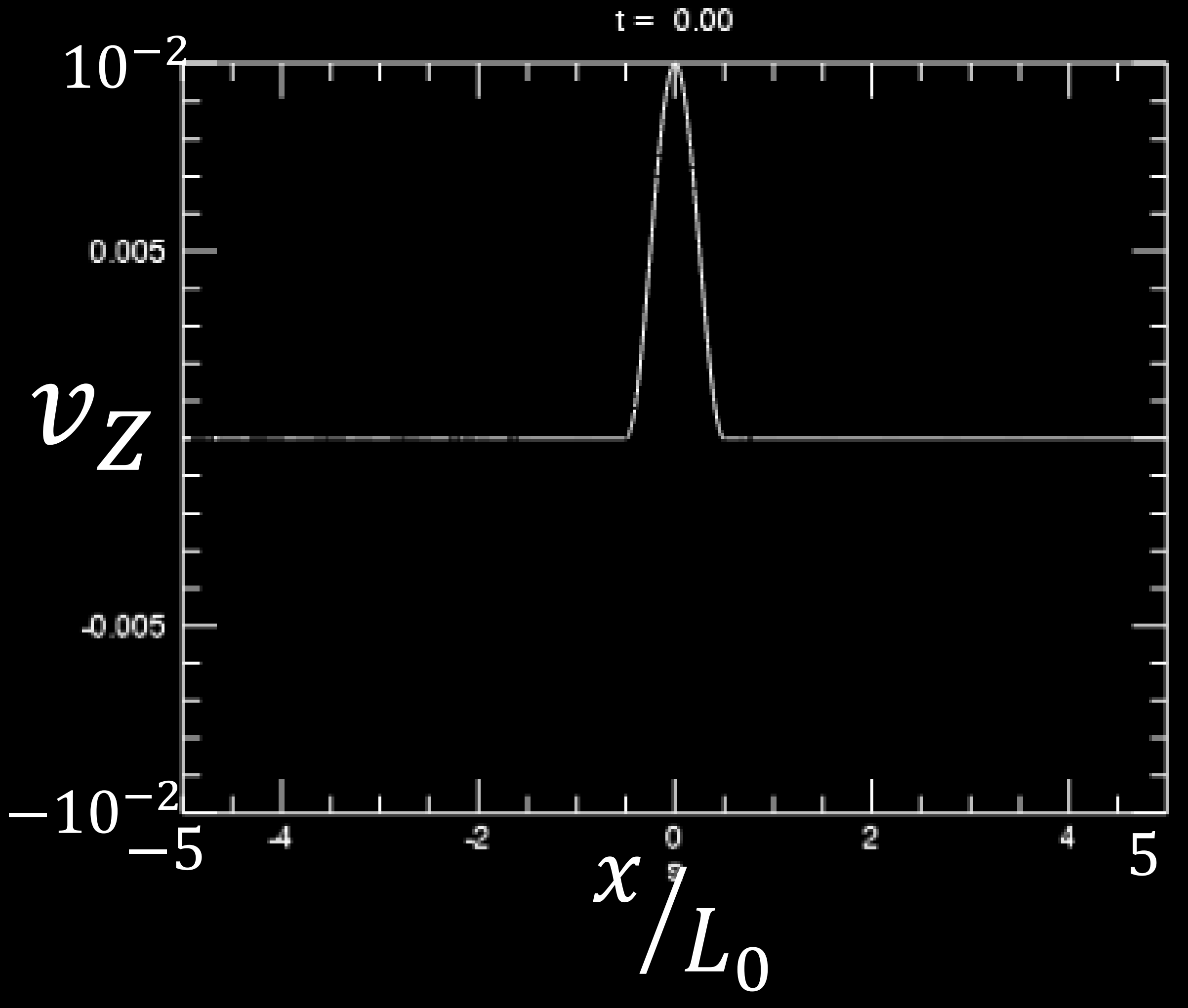

Pondermotive wing

$$B_z = f(\theta) = \epsilon f(x \pm t)$$

$$\frac{\partial}{\partial x} = \frac{d}{d\theta} \quad \frac{\partial}{\partial t} = \pm \frac{d}{d\theta}$$

$$\frac{dv_{||}}{d\theta} \approx \pm \frac{1}{2} \epsilon^2 \frac{\partial B_z^2}{\partial \theta}$$

$$\boxed{v_{||} \approx \pm \frac{1}{2} \epsilon^2 f^2 (x - t) + \mathrm{C}}$$

Cross-Pondermotive Force

$$B_z = \epsilon[f(x+t) + f(x-t)]$$

$$\frac{dv_{||}}{dt} = -\frac{1}{2}\epsilon^2 \frac{\partial}{\partial x}\left[f^2(x+t) + f^2(x-t) + \underbrace{\{f(x-t)f(x+t)\}}_{\text{Cross-Pondermotive Force}}\right]$$

1D Pulse: Summary

- Pondermotive wing:
  - $v_{||} \propto v_z^2$
- Slow waves:
  - Generated by cross-pondermotive force (Verwichte et. al. 1999)

Numerical Experiment: 1D Standing Alfvén Wave

- Uniform $\rho_0, p_0, \boldsymbol{B}_0 = B_0\hat{\boldsymbol{x}}$
- $\boldsymbol{v}_0 = 0$
- Driver at $x = x_{min}$
  - $\frac{v_z}{v_{A0}} = 0.01\sin\left(\frac{\pi t}{t_0}\right)$
- Solid boundary conditions
- $\beta_0 = 0.02$
- Ideal MHD

Numerical Experiment: 1D Standing Alfvén Wave

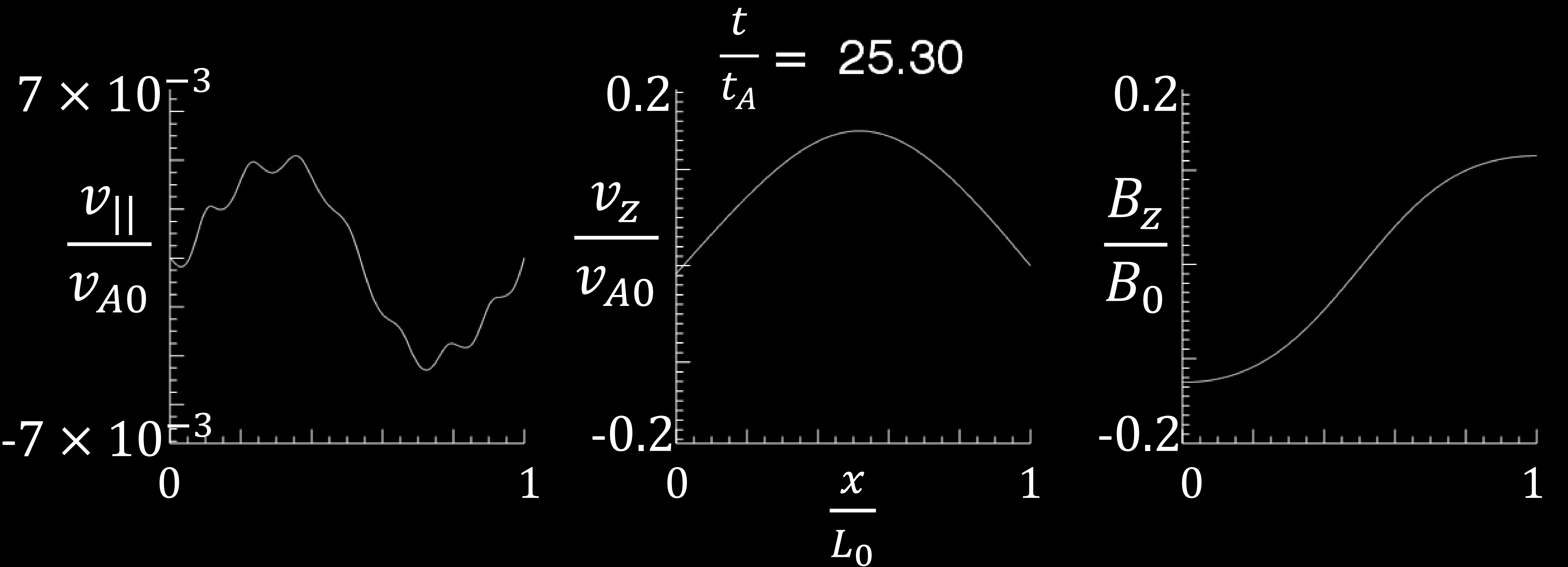

Numerical Experiment: 1D Standing Alfvén Wave

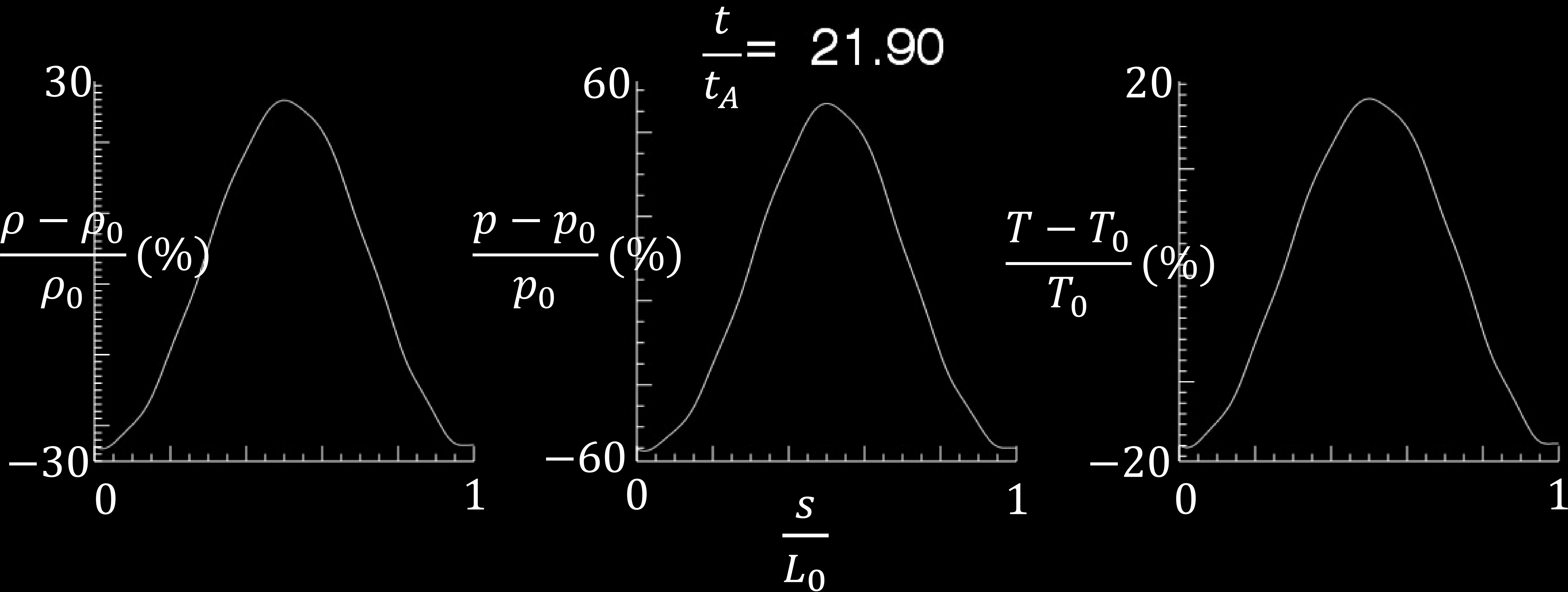

Density Enhancement

If: $v_z \sim \epsilon \sin x \sin t$

Then: $\rho \sim \rho_0 + \frac{1}{4}\epsilon^2 t^2 \cos 2x \qquad (\beta = 0)$

$$\rho \sim \rho_0 + \frac{1}{4}\frac{\epsilon^2}{c_s^2}\sin^2 c_s t \cos 2x \qquad (\beta \neq 0)$$

Beating Effect

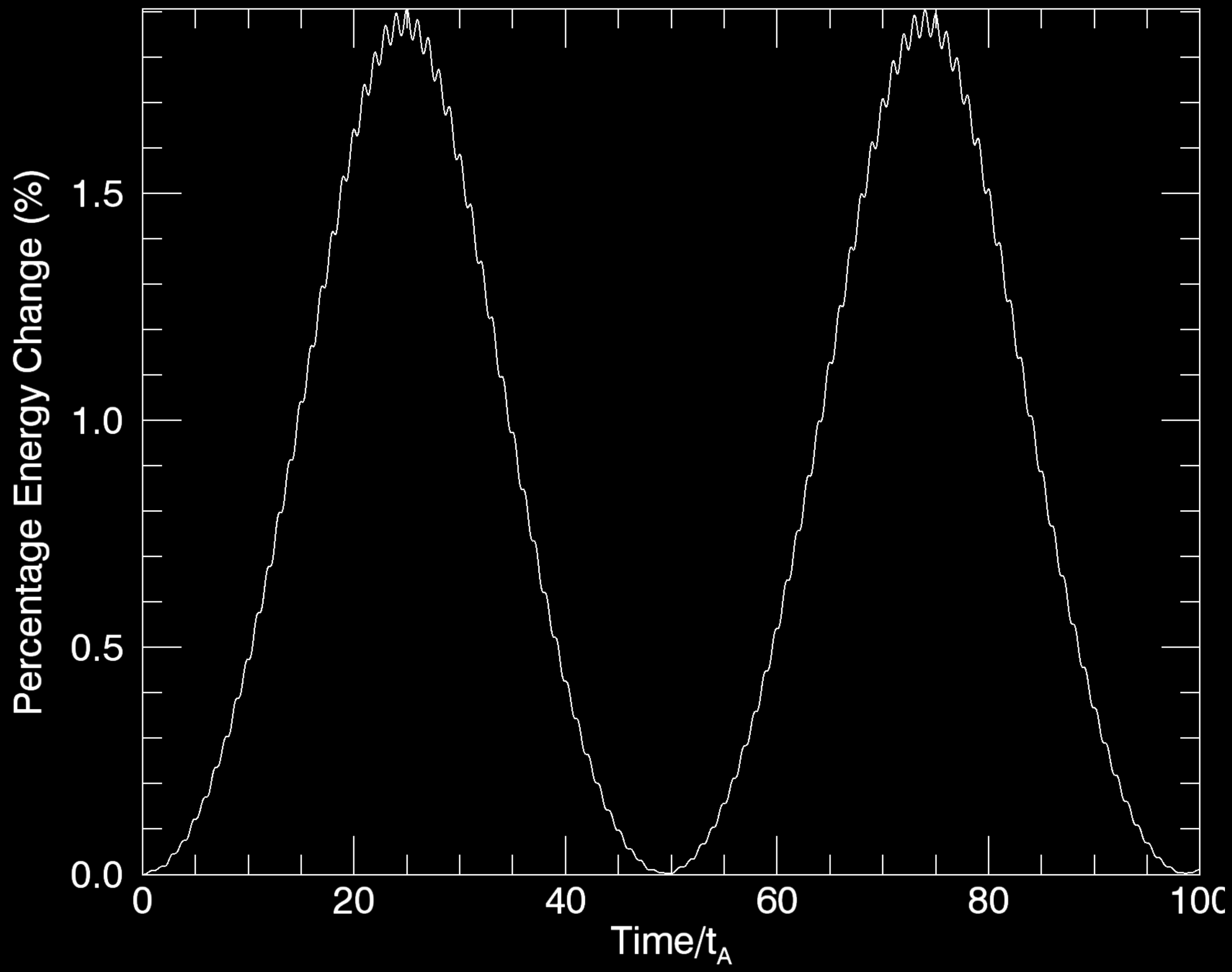

Why does temperature increase / decrease occur?

- Gas evolves adiabatically

$$p_1 = v_s^2 \rho_1$$

$$\frac{T_1}{T_0} \approx (\gamma - 1)\frac{\rho_1}{\rho_0}$$

- If isothermal:
  - Negligible effect on pressure enhancement
  - Density enhancement increases by a factor γ

1D Standing Wave: Summary

- Density increase/decrease occurs at antinodes/nodes of v_z
- Increasing β decreases amplitude in density
- Thermal conduction acts to increase the amplitude in density

2D X-point Field: Setup

- Uniform ρ_0, p_0
- $\boldsymbol{B}_0 = \frac{B_{norm}}{L_0}\,(x, -y)$
- $\boldsymbol{v}_0 = 0$

- $\rho_0 = 1.67 \times 10^{-12}\mathrm{kgm}^{-3}$
- $B_{norm} = 2.5 \times 10^{-3}\mathrm{T}$
- $L_0 = 1\mathrm{Mm}$
- $T_0 \approx 9 \times 10^5\mathrm{K}$

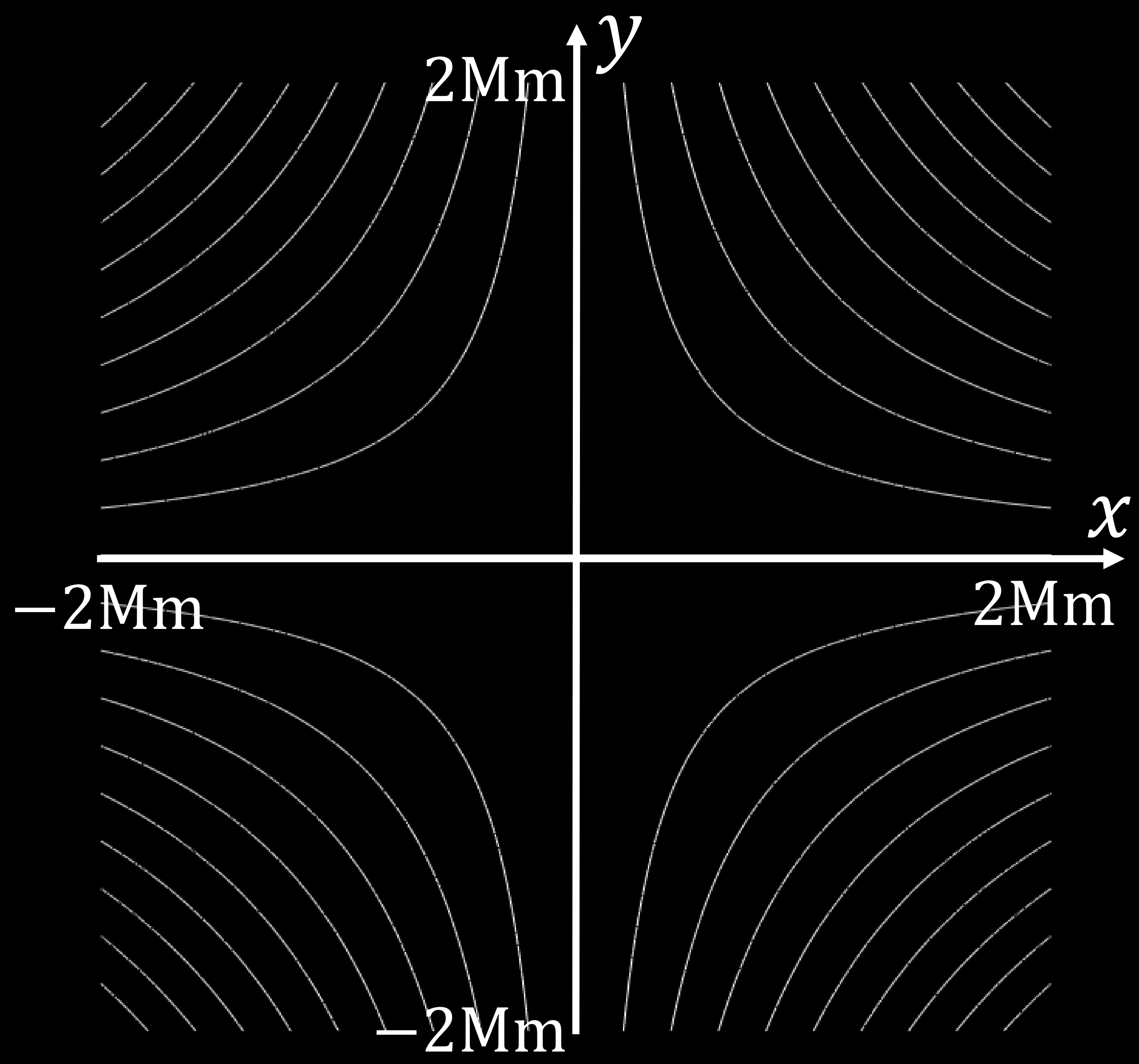

2D X-point Field: Plasma Beta

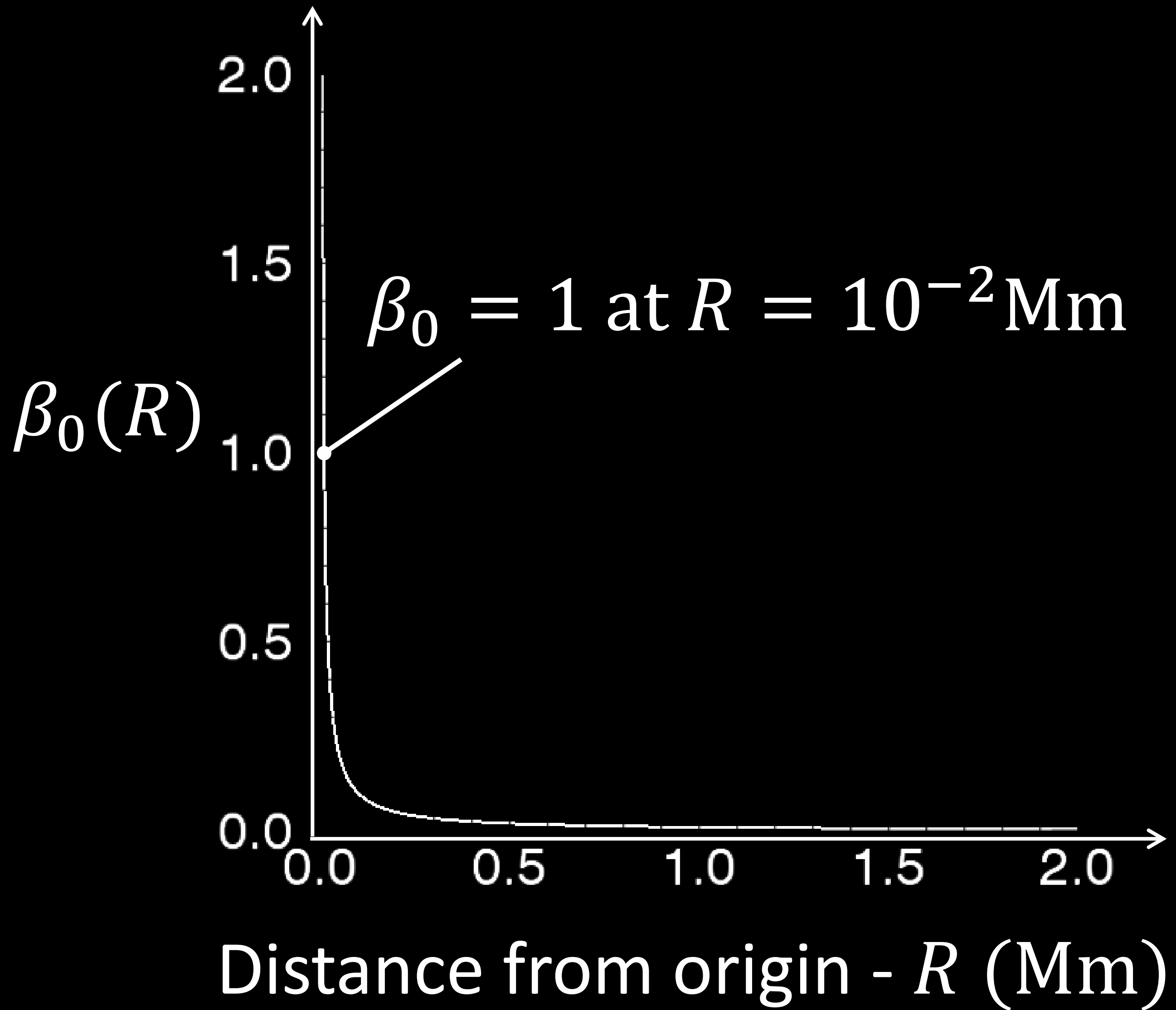

2D X-point Field: Boundary Conditions

- Driver at $y = y_{min}$ with spatial profile illustrated
- Time profile: $\sin\left(\frac{\pi t}{\ln(4) t_0}\right)$
- Solid boundary conditions

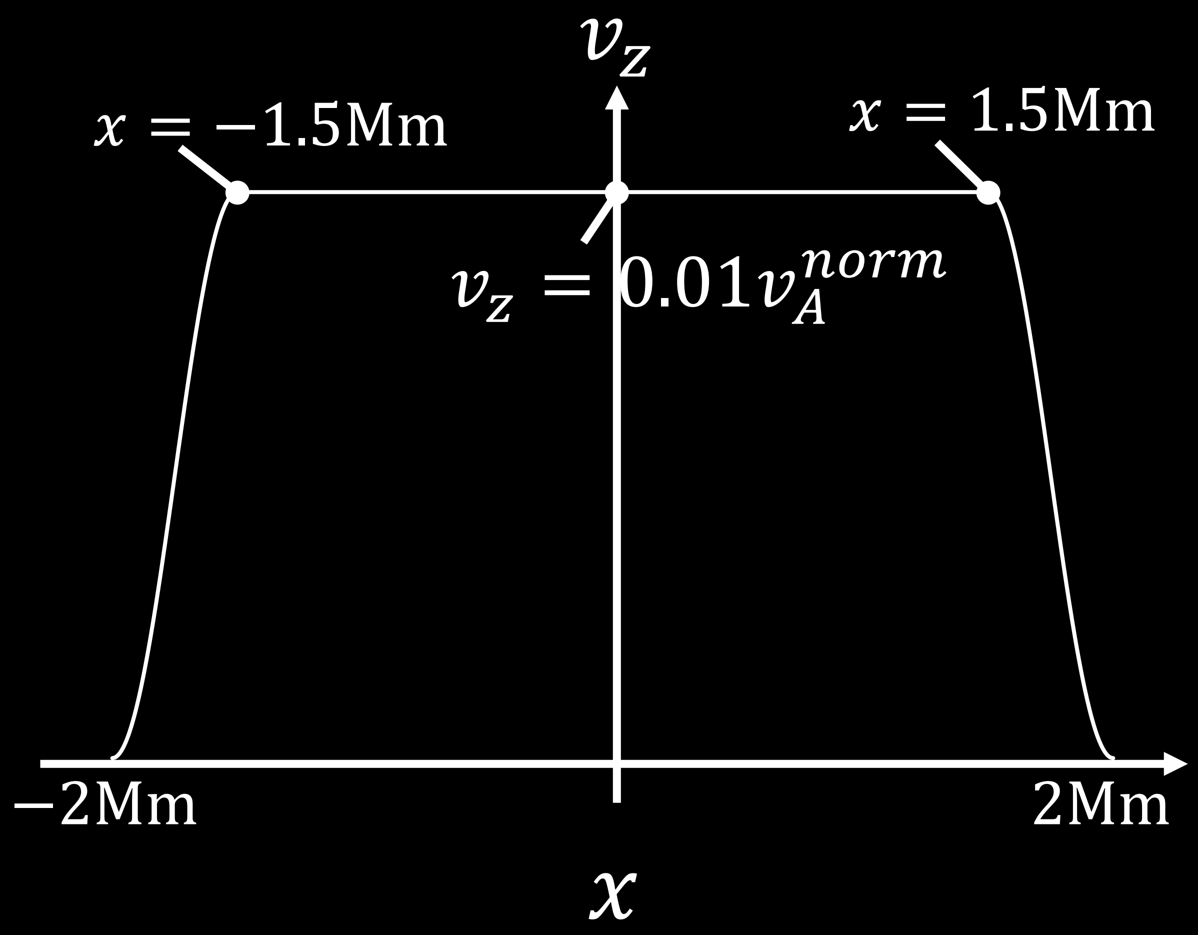

2D X-point Field: Thermal conduction

- Implemented by solving:

$$\rho \frac{\partial \epsilon}{\partial t} = \nabla \cdot \left(\left(\kappa_0 T^{\frac{5}{2}} \frac{\boldsymbol{B}}{B^2 + b_{min}^2} \cdot \nabla T \right) \boldsymbol{B} \right) + \nabla \cdot \left(\kappa_0 T^{5/2} \frac{b_{min}}{B^2 + b_{min}^2} \nabla T \right)$$

- $b_{min} = 0$ recovers Braginskii thermal conduction:

$$\rho \frac{\partial \epsilon}{\partial t} = \nabla \cdot \left(\kappa_0 T^{5/2} \left(\widehat{\boldsymbol{B}} \cdot \nabla T \right) \widehat{\boldsymbol{B}} \right)$$

- $b_{min} = 10^{-6} B_{norm}$

2D X-point Field: Setup

- $\eta \neq 0$
- ${}^{\tau_{cond_0}}/_{T_D} \approx 1.6,$
- $t_{end} \approx 15T_D$
- No viscosity

Numerical Experiment: 2D X-point Field

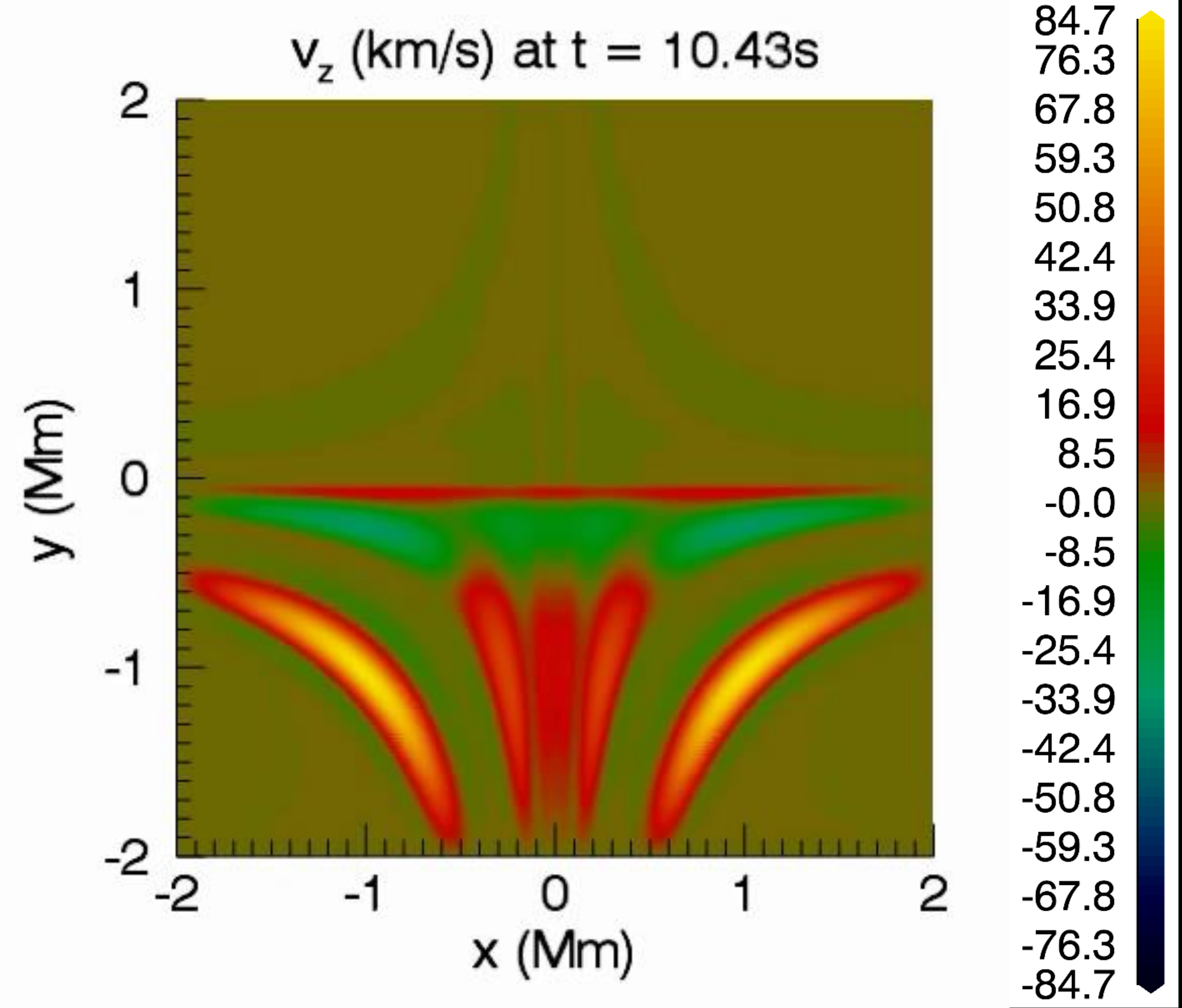

$v_A^{norm} \approx 1.73 \times 10^6 \mathrm{ms}^{-1}$

$84.7\mathrm{kms}^{-1} \approx 0.05 v_A^{norm}$

$\text{Driver Amplitude} = 0.01 v_A^{norm}$
$\approx 16.94\mathrm{km/s}$

Numerical Experiment: 2D X-point Field

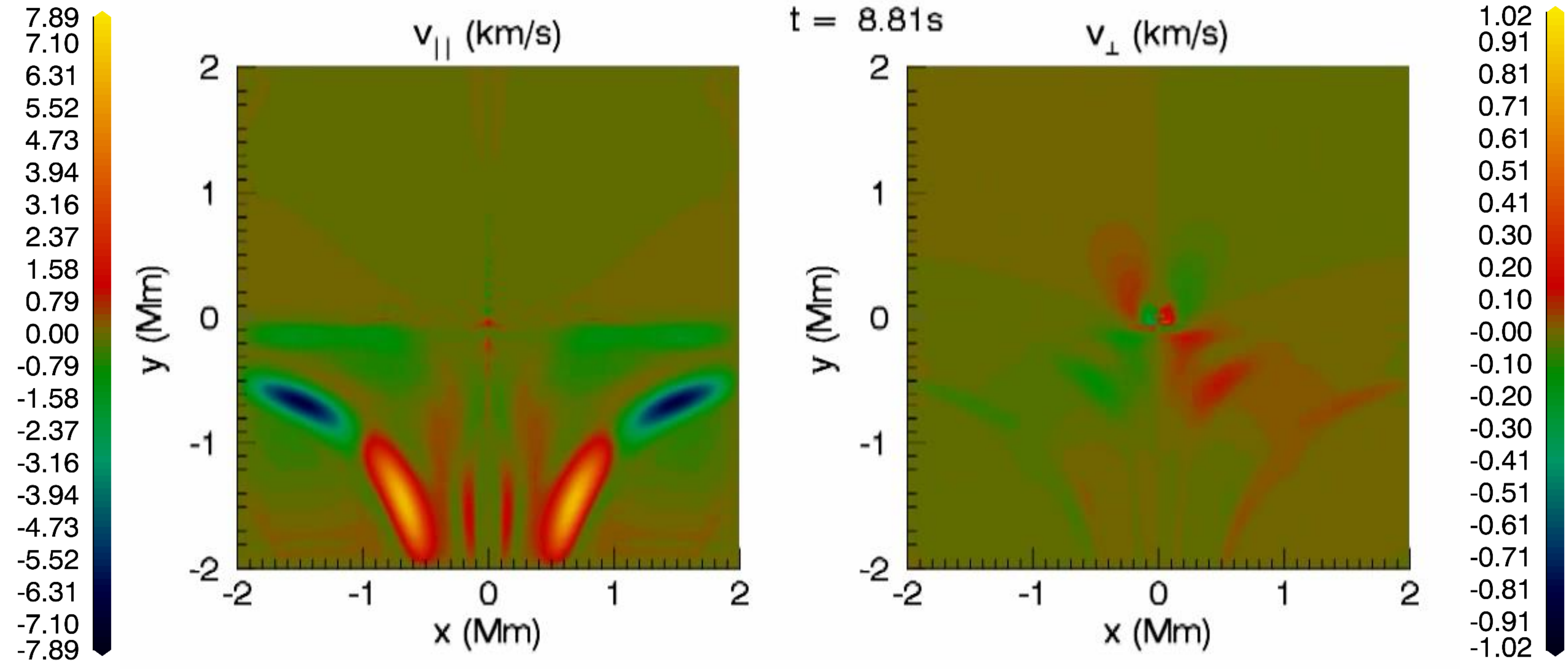

For $\beta \ll 1$: $v_{||} \rightarrow$ Slow waves and pondermotive wings

$v_{\perp} \rightarrow$ Fast waves

Numerical Experiment: 2D X-point Field

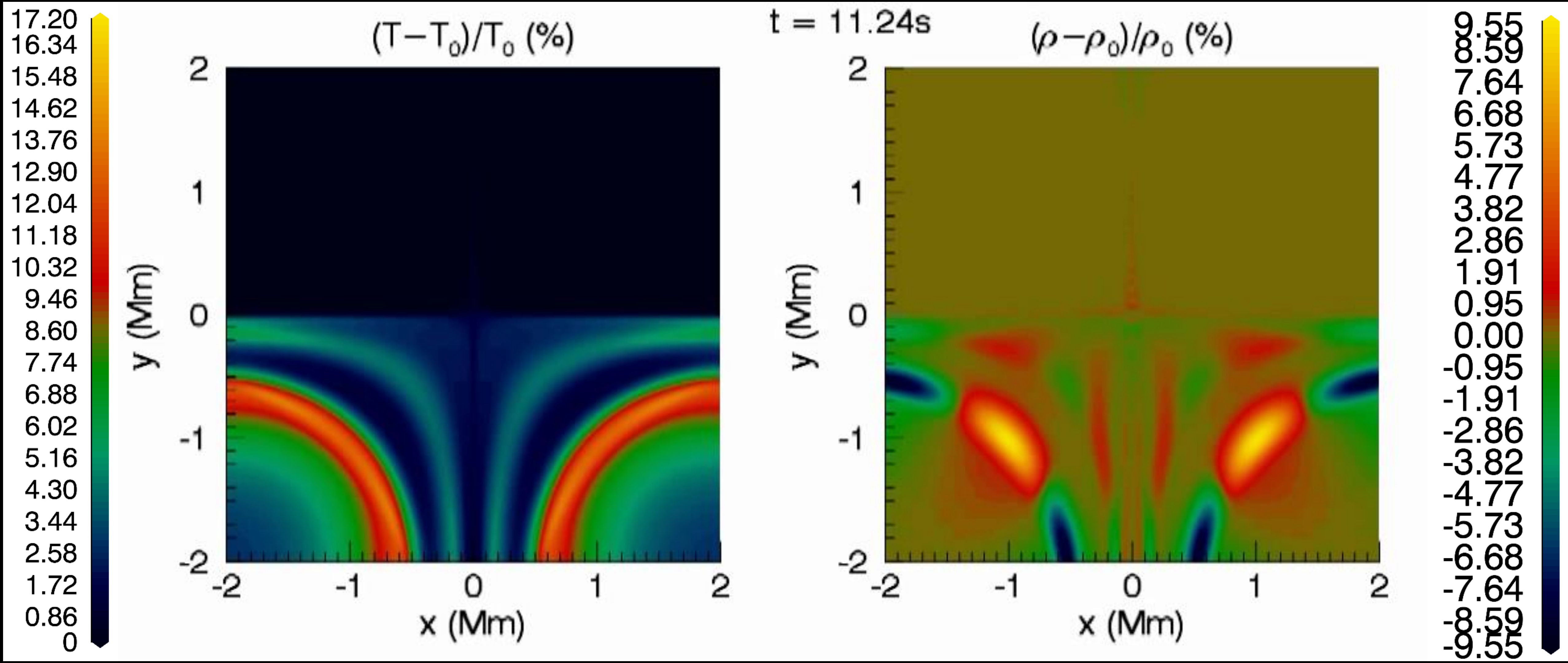

Resonance

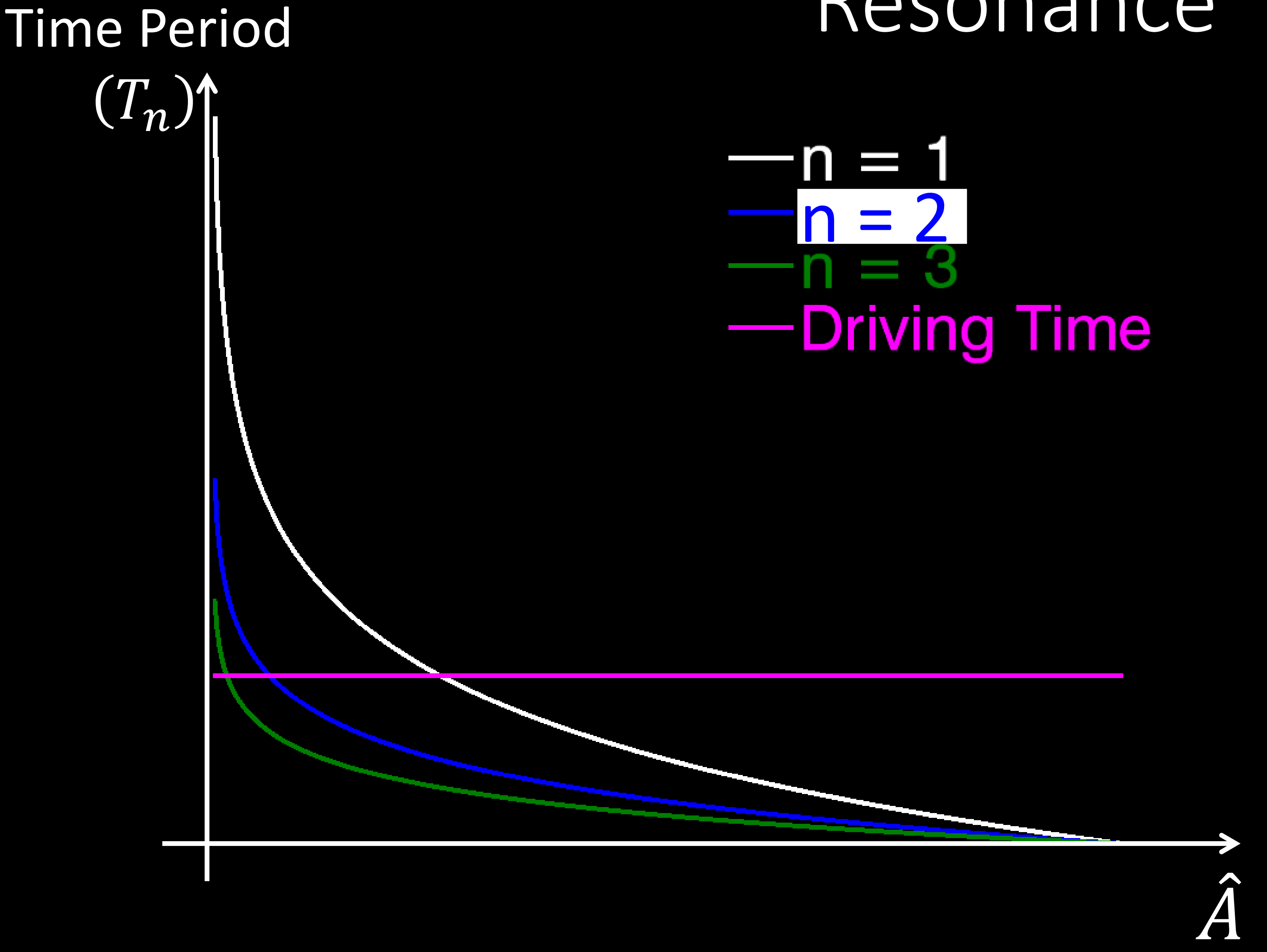

$$T_n = \frac{2}{n}\tau_{A0}\ln\left(\frac{\hat{x}_{max}\,\hat{y}_{max}}{\hat{A}}\right)$$

For $\hat{A} = \hat{x}\hat{y}$

Why do the resonating field lines further from the origin have more energy?

$$|v_A| \propto R$$

$$\Longrightarrow \frac{\delta v_A}{v_{A0}} \propto \frac{1}{R}$$

$$\Longrightarrow \delta T_n \propto \frac{1}{R}$$

$\Longrightarrow$ Beating Time Period $\propto R$

Current Sheet Formation

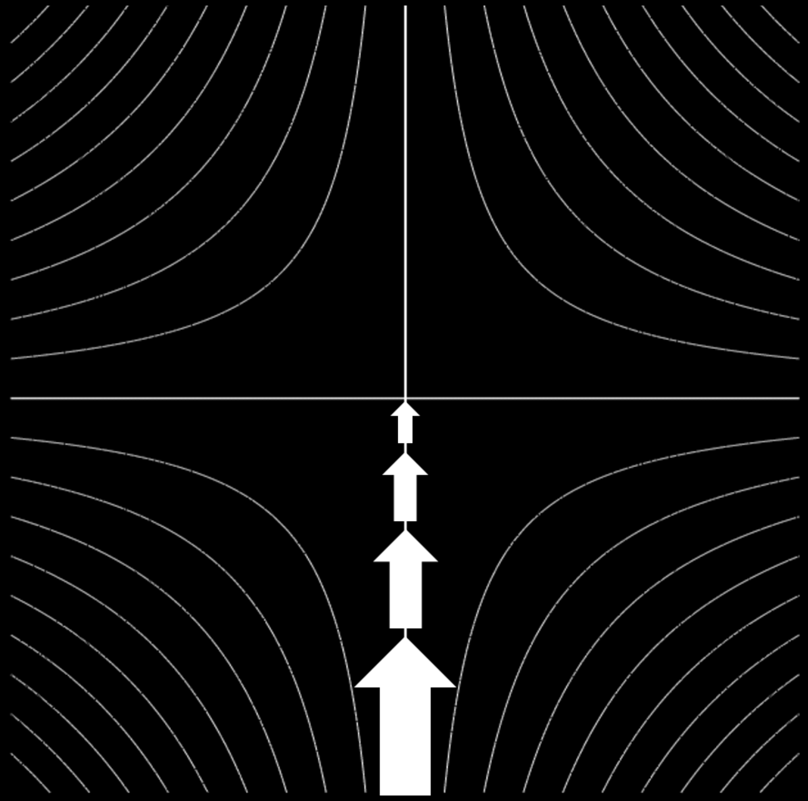

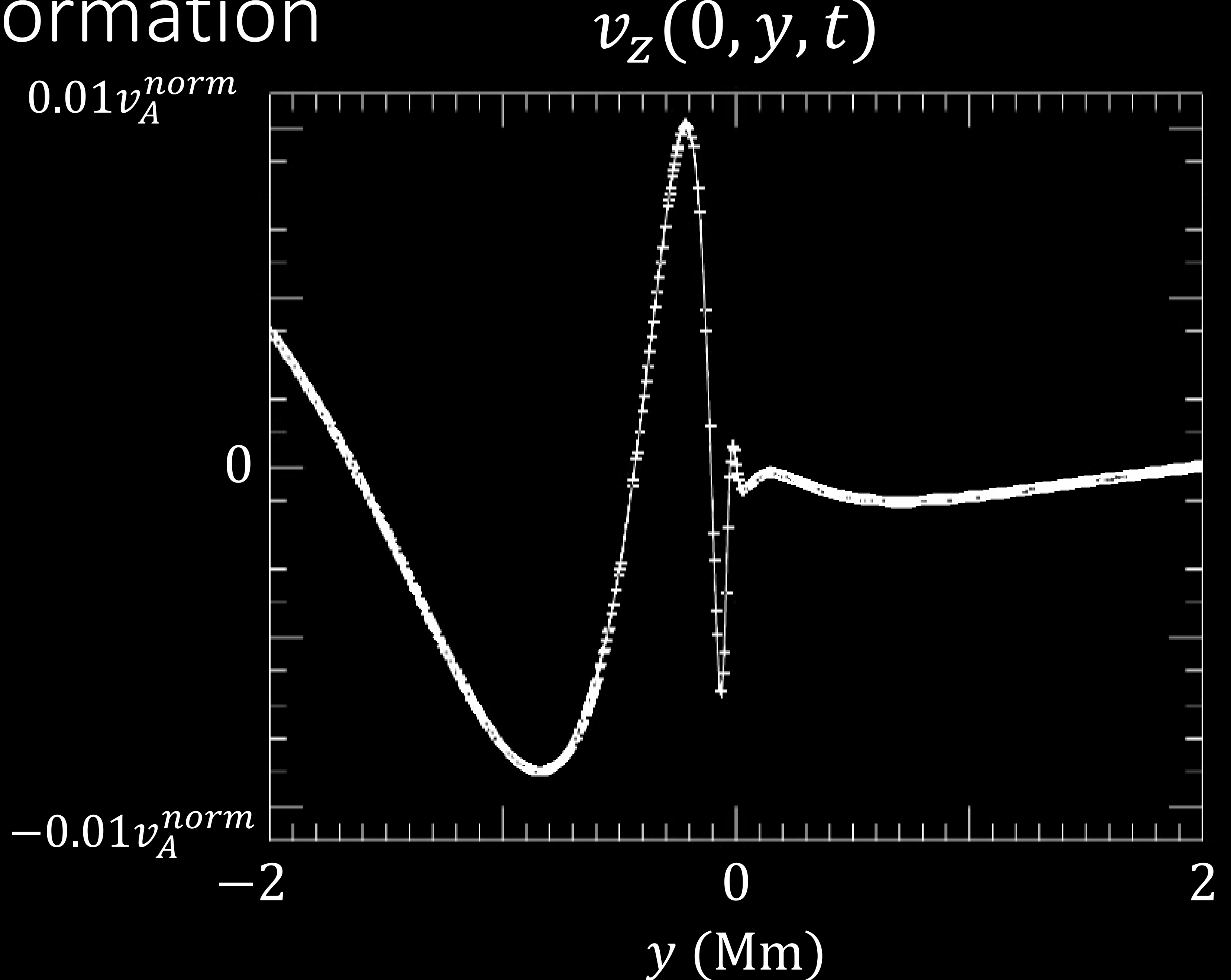

How is magnetic energy converted to heat?

Magnetic Diffusion

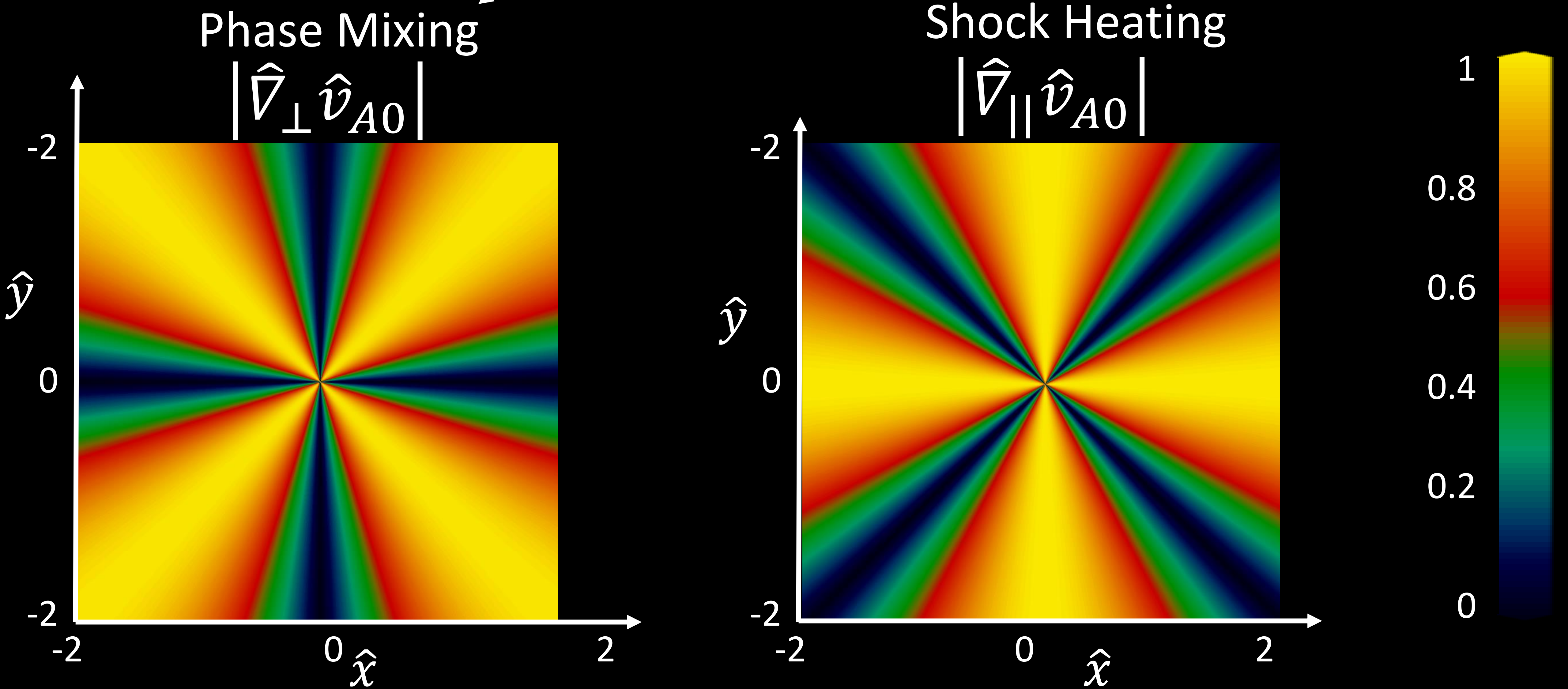

$\sqrt{jx^2 + jy^2 + jx^2}$ (mA) at $t = 11.24$s

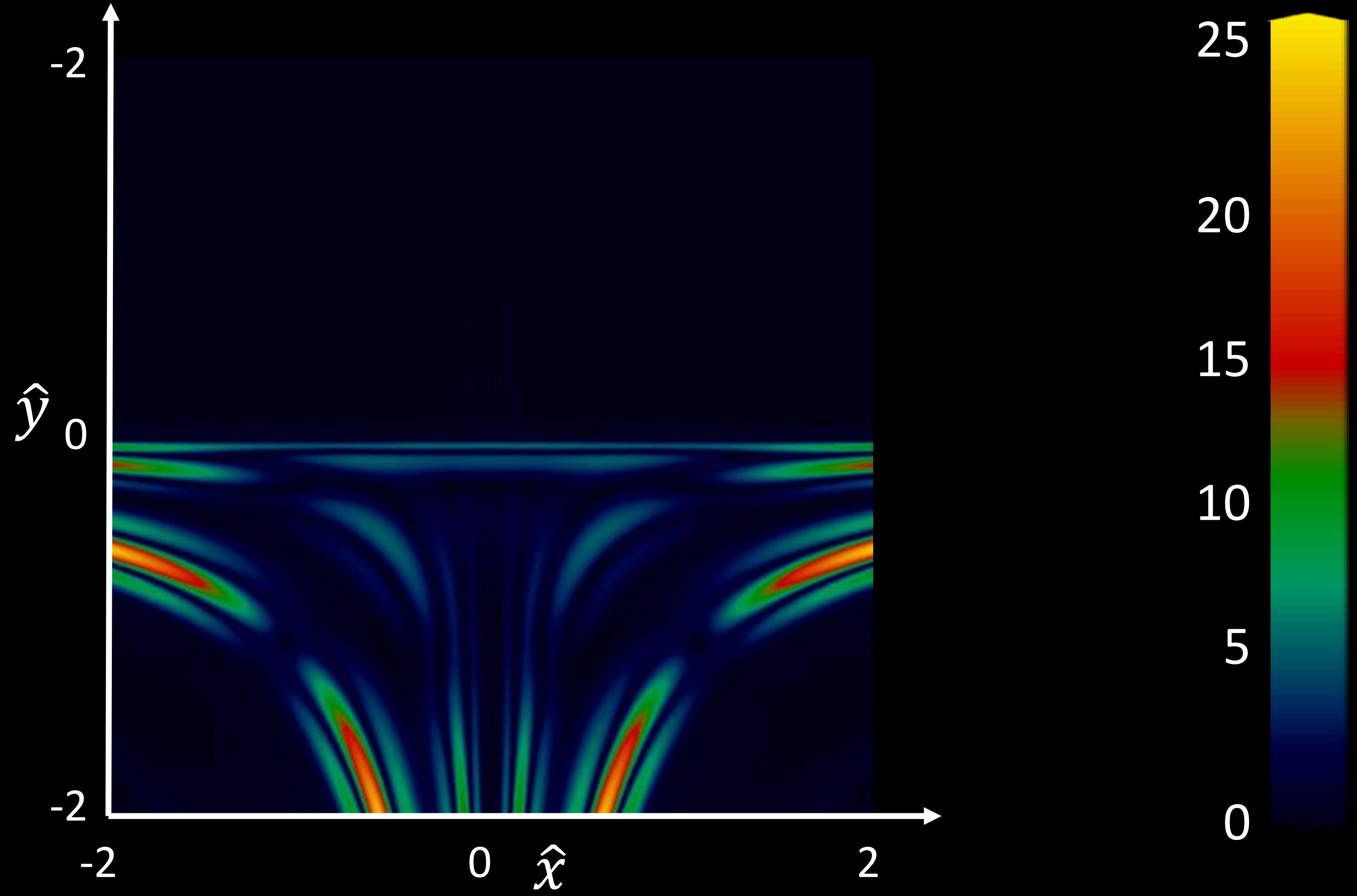

$v_{||}$ along $x = 0$ (km/s)

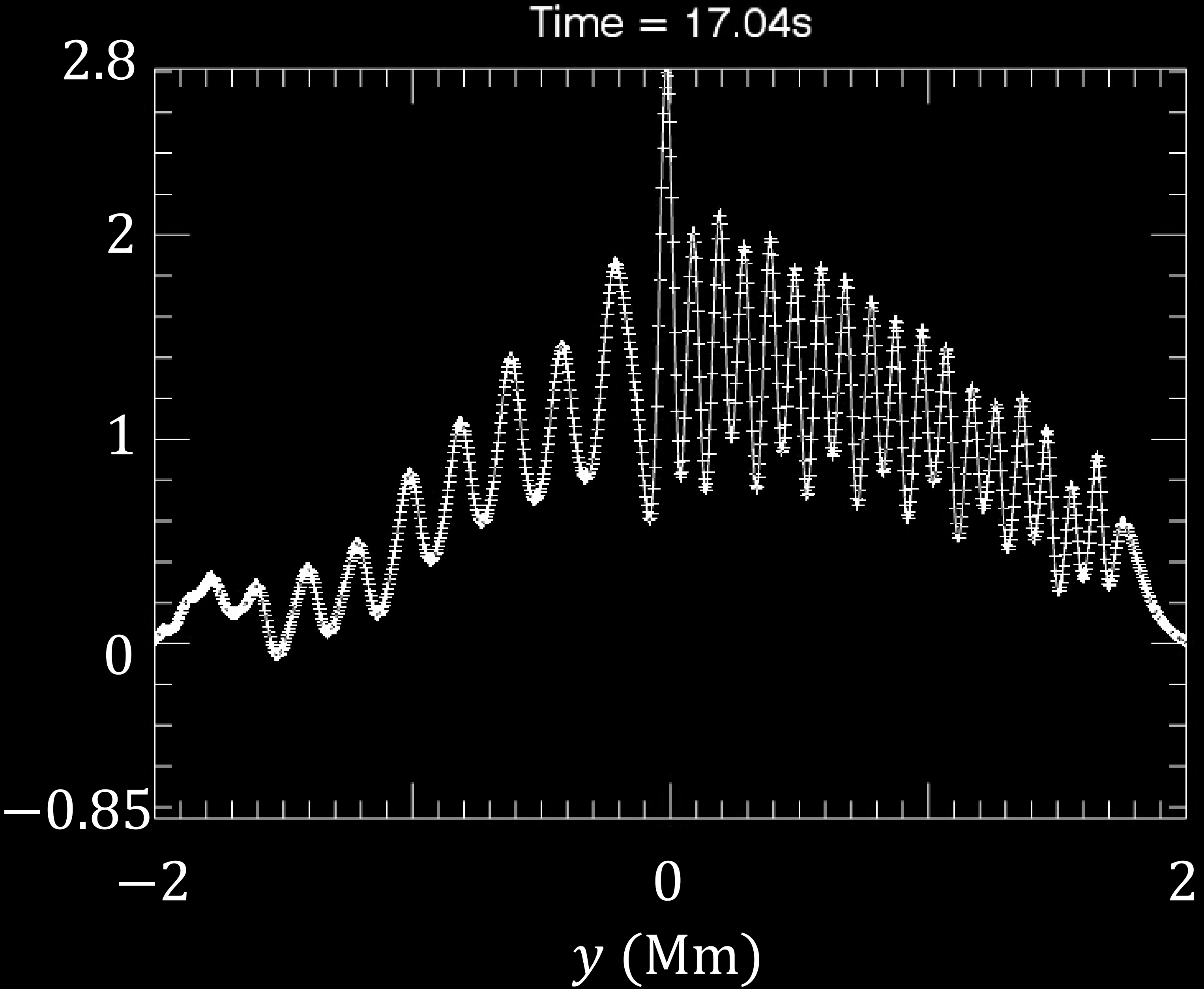

McLaughlin 2009 and Santamaria et. al. 2017 have qualitatively similar results

Santamaria Results

Longitudinal Acoustic Energy $\sim v_{||}$

Pressure

Transverse Magnetic Energy $\sim v_{\perp}$

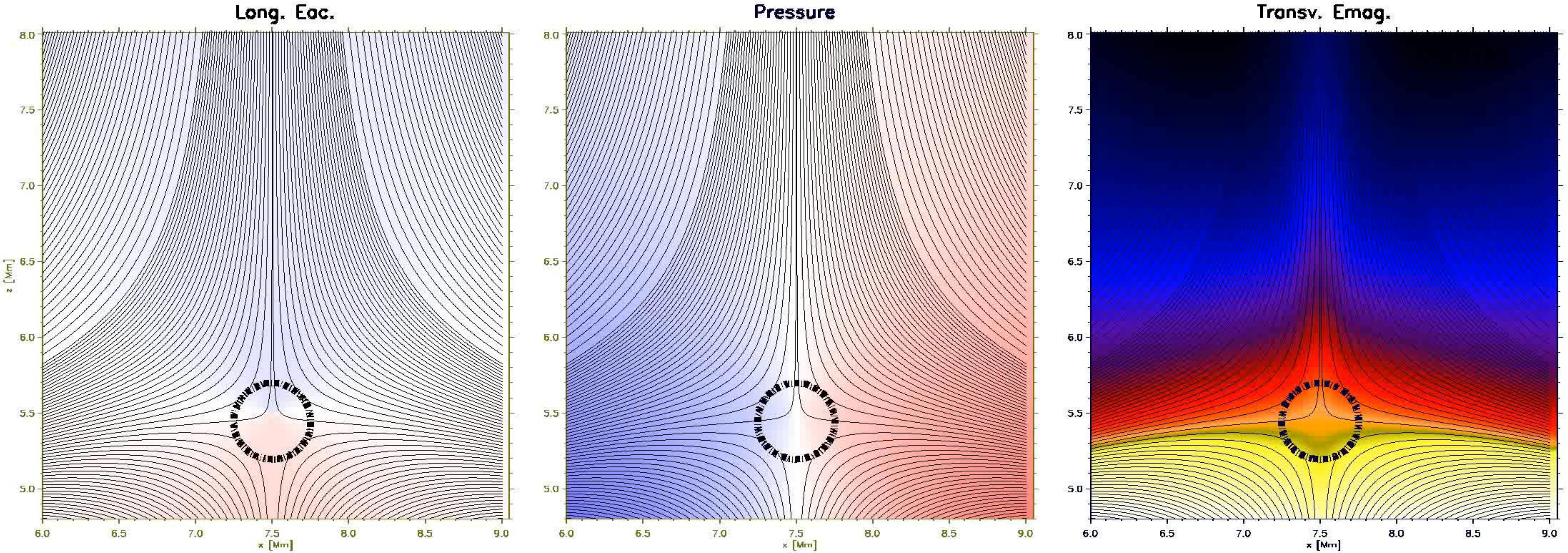

z-Energy (E_z) Leakage

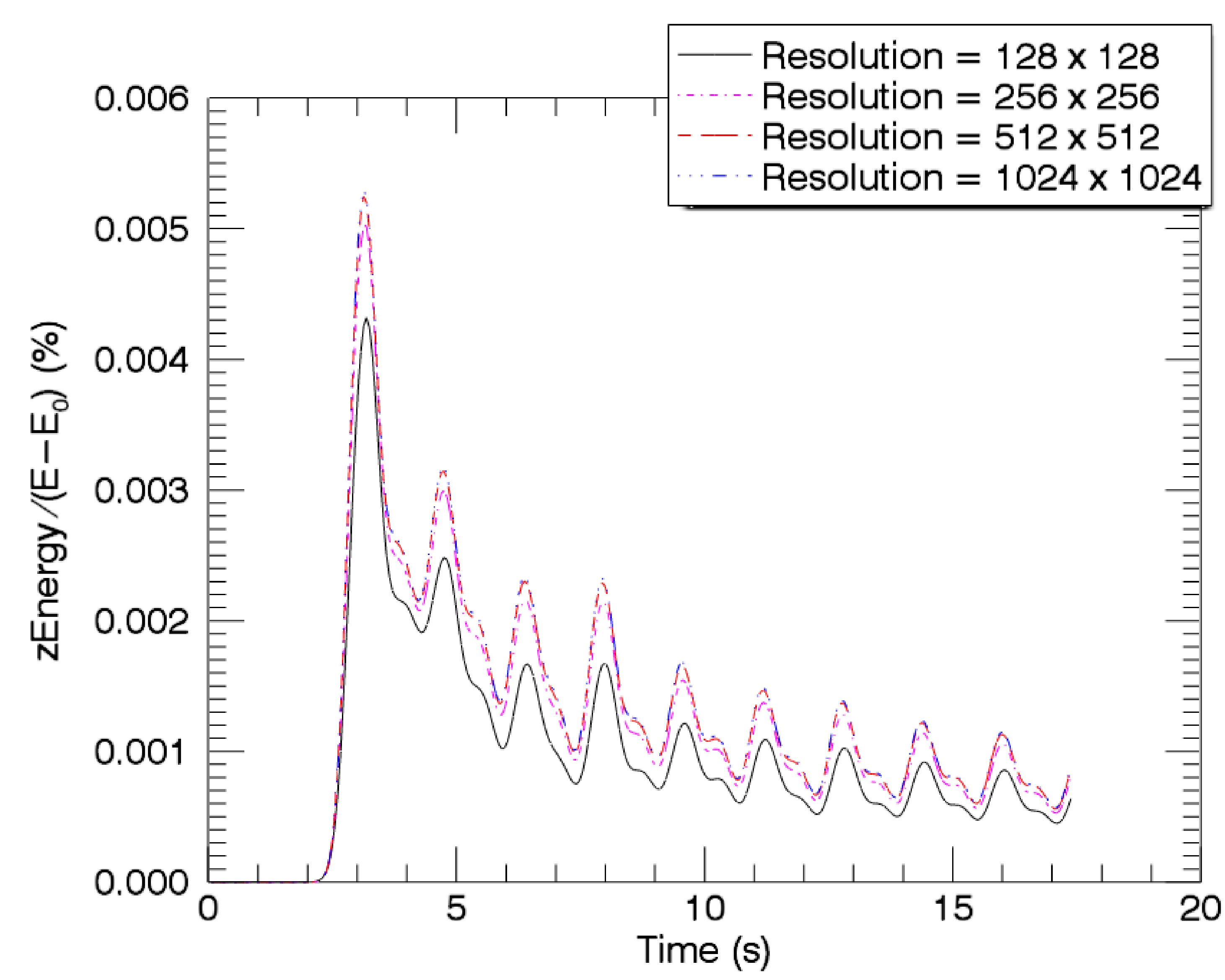

$$E_z = \int_A \frac{B_z^2}{2\mu_0} + \frac{1}{2}\rho v_z^2 dS$$

Where A is the top half of the domain

Summary

- Alfven waves generate pondermotive wings, slow waves and fast waves
- Standing Alfven waves generate standing density and pressure waves with half the wavelength
- Standing Alfven waves on an x-point field are damped by phase mixing
- Complex MHD coupling at occurs as MHD waves cross the $\beta = 1$ circle around a null point

Future Work

- Study MHD waves in more realistic configurations
- Study the behaviour of MHD waves as they cross the $\beta = 1$ circle around a null point

$$B_x = \sin x \ e^{-y}$$
$$B_y = 1 - \cos x \ e^{-y}$$

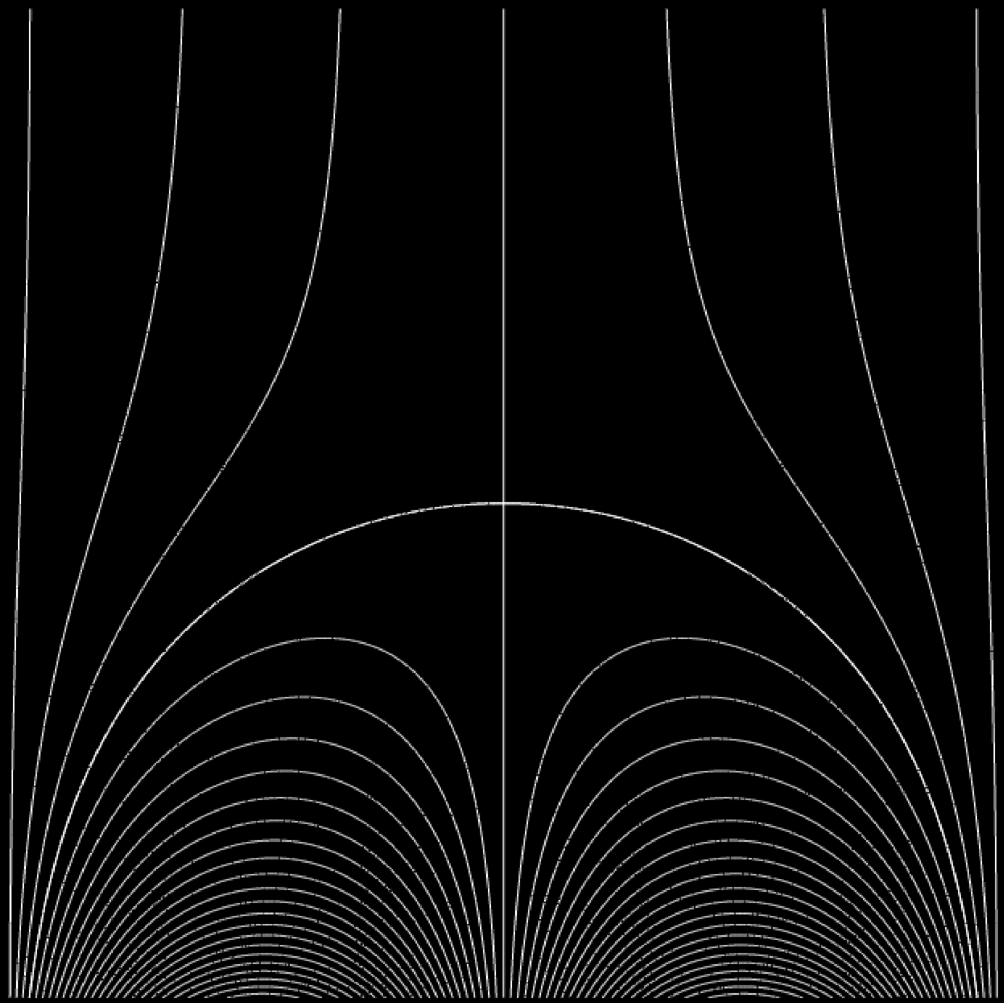

References

McLaughlin, J. 2016. Behaviour of magnetoacoustic waves in the neighbourhood of a two-dimensional null point: Initially cylindrically symmetric perturbations. *Journal of Astrophysics and Astronomy*, 37(1):2.

McLaughlin, J. A., I. De Moortel, A. W. Hood, and C. S. Brady 2009. Nonlinear fast magnetoacoustic wave propagation in the neighbourhood of a 2d magnetic x-point: oscillatory reconnection. *Astronomy & Astrophysics*, 493(1):227–240.

Santamaria, I., E. Khomenko, M. Collados, and A. de Vicente 2017. High-frequency waves in the corona due to null points. *Astronomy & Astrophysics*, 602:A43.

Terradas, J. and L. Ofman 2004. Loop density enhancement by nonlinear magnetohydrodynamic waves. *The Astrophysical Journal*, 610(1):523.

Thurgood, J. and J. McLaughlin 2013. On ponderomotive effects induced by alfven waves in inhomogeneous 2.5 d mhd plasmas. *Solar Physics*, 288(1):205–222.

Tomczyk, S., S. McIntosh, S. Keil, P. Judge, T. Schad, D. Seeley, and J. Edmondson 2007. Alfvén waves in the solar corona. *Science*, 317(5842):1192–1196.

Verwichte, E., V. Nakariakov, and A. Longbottom 1999. On the evolution of a nonlinear alfvén pulse. *Journal of plasma physics*, 62(2):219–232.